PHYSICS AND CHEMISTRY OF SOLID STATE
V. 21, No. 3 (2020) pp. 530-536

Vasyl Stefanyk Precarpathian National University

ФІЗИКА І ХІМІЯ ТВЕРДОГО ТІЛА
Т. 21, № 3 (2020) С. 530-536

DOI: 10.15330/pcss.21.3.530-536

UDC 680.18:669.71

ISSN 1729-4428

O.V. Sukhova, V.A. Polonskyy

Peculiarities in Structure Formation and Corrosion of Cast Quasicrystalline $Al_{63}Cu_{25}Fe_{12}$ and $Al_{63}Co_{24}Cu_{13}$ Alloys in Sodium Chloride Aqueous Solution

The Oles' Honchar Dniprovs'k National University, Dnipro, Ukraine, sukhovaya@ukr.net

In this work the structure and corrosion behavior of quasicrystalline cast $Al_{63}Cu_{25}Fe_{12}$ and $Al_{63}Co_{24}Cu_{13}$ alloys in 5 % sodium chloride solution (pH 6.9 - 7.1) were investigated. The alloys were cooled at 5 K/s. The structure of the samples was studied by methods of quantitative metallography, X-ray analysis, and scanning electron microscopy. Corrosion properties were determined by potentiodynamic method. The made investigations confirm the formation of stable quasicrystalline icosahedral (ψ) and decagonal (D) phases in the structure of $Al_{63}Cu_{25}Fe_{12}$ and $Al_{63}Co_{24}Cu_{13}$ alloys correspondingly. In 5 % sodium chloride solution, the investigated alloys corrode under electrochemical mechanisms with oxygen depolarization. Compared with $Al_{63}Cu_{25}Fe_{12}$ alloy, $Al_{63}Co_{24}Cu_{13}$ alloy has less negative value of free corrosion potential (–0.43 V and –0.66 V, respectively), and its electrochemical passivity region extends due to the inhibition of anodic processes. A corrosion current density, calculated from (E,lgi)-curve, for $Al_{63}Co_{24}Cu_{13}$ alloy amounts to 0.18 mA/cm^2 and for $Al_{63}Cu_{25}Fe_{12}$ alloy – to 0.20 mA/cm^2. The lower corrosion resistance of $Al_{63}Cu_{25}Fe_{12}$ alloy may be explained by the presence of iron-containing phases in its structure. Based on obtained results, the $Al_{63}Co_{24}Cu_{13}$ alloy was recommended as coating material for rocket-and-space equipment working in marine climate.

Keywords: icosahedral quasicrystals, decagonal quasicrystals, structure, electrochemical polarization, pitting corrosion.

Received 30 April 2020; Accepted 15 September 2020.

Introduction

The Al–Cu–Fe and Al–Cu–Co alloy systems containing stable quasicrystalline phases are the most interesting functional materials. The interest also is prompted due to the finding of quasicrystalline phases of the above alloys when they are cast under conventional solidification techniques. Three-dimensional Al–Cu–Fe quasicrystals show a five-fold symmetry and have icosahedral structure [1, 2]. The Al–Cu–Co quasicrystals are two-dimensional decagonal quasicrystals consisting of periodic stacking of atomic layers with a tenfold symmetry within the plane [3, 4]. Thus, decagonal quasicrystals combine two types of crystalline order: they are quasiperiodic in a plane and they are periodic in the direction perpendicular to a plane. This property sets decagonal phases apart from periodic crystals, as well as from icosahedral quasicrystals.

Quasicrystalline Al–Cu–Fe and Al–Cu–Co alloys may be used as structural components in rocket-and-space industry owing to their high hardness, low surface energy, high wear resistance, low friction, and resistance to oxidation [5-11]. But the quasicrystalline alloys cannot be applied as functional materials due to their brittle nature at ambient temperature. However, the combination of excellent physical and mechanical properties makes them the promising material for surface application as thick composite [12-15] and ion-plasma thin coatings [16-21] when good corrosion resistance is additionally required.

The rocket-and-space equipment has been currently operating in marine climate, where salt may affect component surface. Therefore, it is interesting to compare the resistance to corrosion as well as the electrochemical behavior of quasicrystalline cast icosahedral Al–Cu–Fe and decagonal Al–Cu–Co

quasicrystals in sodium chloride aqueous solution.

I. Experimental procedure

The $Al_{63}Cu_{25}Fe_{12}$ and $Al_{63}Co_{24}Cu_{13}$ alloys were prepared of high purity (99.99 %) components put in a graphite crucible and melted using Tamman furnace. The cooling rate of the alloys was 5 K/s. In order to verify the bulk compositions, *Sprut СЕФ-01-М* atomic absorption spectroscopy instrument was applied for the examination of selected samples. The relative precision of the measurements was better than ± 1 at. %.

The instruments used in the microstructural characterization of the investigated alloys were mainly *Neophot* and *GX-51* optical microscopes (OM), *Epiquant* quantitative analyzer, *РЭМА 102-02* scanning electron microscope (SEM). The alloys were also studied by powder X-ray diffraction (XRD) using *ДРОН-УМ-1* diffractometer with CuK_α radiation. Vickers hardness measurements were carried out at indentation load of 50 g. The data shown was an average of at least 5 measurements.

Electrochemical experiments were conducted in 5 % aqueous sodium chloride solution (pH = 6.9 - 7.1) by means of *ПИ–50–1* potentiostat and *ПР–8* programmer using three-electrode electrolytic system consisted of silver chloride as reference electrode, a platinum as counter electrode, and the sample as working electrode. Potentiodynamic measurements were carried out by sweeping the potential in the positive or negative direction with a sweep rate of 1 mV/s until a current limit in the mA range was reached.

Model corrosion tests for 1, 2, 3, 4, 8 days in a 5 % NaCl solution were performed with specimens 3.0×0.5 cm in size. The specimens were fully immersed in the saline solution. Testing under these conditions was assumed to be equivalent to a 5-years application in sea atmosphere. The surface morphology was examined using a scanning electron microscope (SEM). Corrosion and electrochemical tests were carried out at the temperature of 293 ± 2 K.

II. Experimental results and discussion

The $Al_{63}Cu_{25}Fe_{12}$ alloy exhibits multiphase microstructure (Fig. 1, a,b) [2]. The primary λ-$Al_{13}Fe_4$ phase is nucleated directly from the melt and grows into the liquid, and the β-AlFe(Cu) phase is formed directly from the liquid or via a peritectic reaction between the primary λ and liquid. The λ-phase is surrounded by a shell of the quasicrystalline icosahedral ψ-Al_6Cu_2Fe phase that is formed afterward via peritectic reaction. The peritectic reaction does not go to completion and the remaining liquid solidifies into low-temperature metastable crystalline phases such as τ-AlCu(Fe), η-AlCu, and θ-Al_2Cu. The phase constitution of the as-cast $Al_{63}Cu_{25}Fe_{12}$ alloy is also confirmed by XRD pattern (Fig. 1, c). The diffractogram indicates that the ψ and λ phases are dominant. Their volume fraction measured by quantitative metallography amounts to 55.5 and 32.0 vol.% respectively. Furthermore, several weaker reflections of minor phases can be seen in the diffractogram as well. The XRD pattern is not suitable to distinguish the τ and η phases in the solidification product, since they have similar CsCI-type cubic structure and lattice parameter [1].

Examination by light-optical microscopy reveals that $Al_{63}Co_{24}Cu_{13}$ alloy consists of three phases identified as

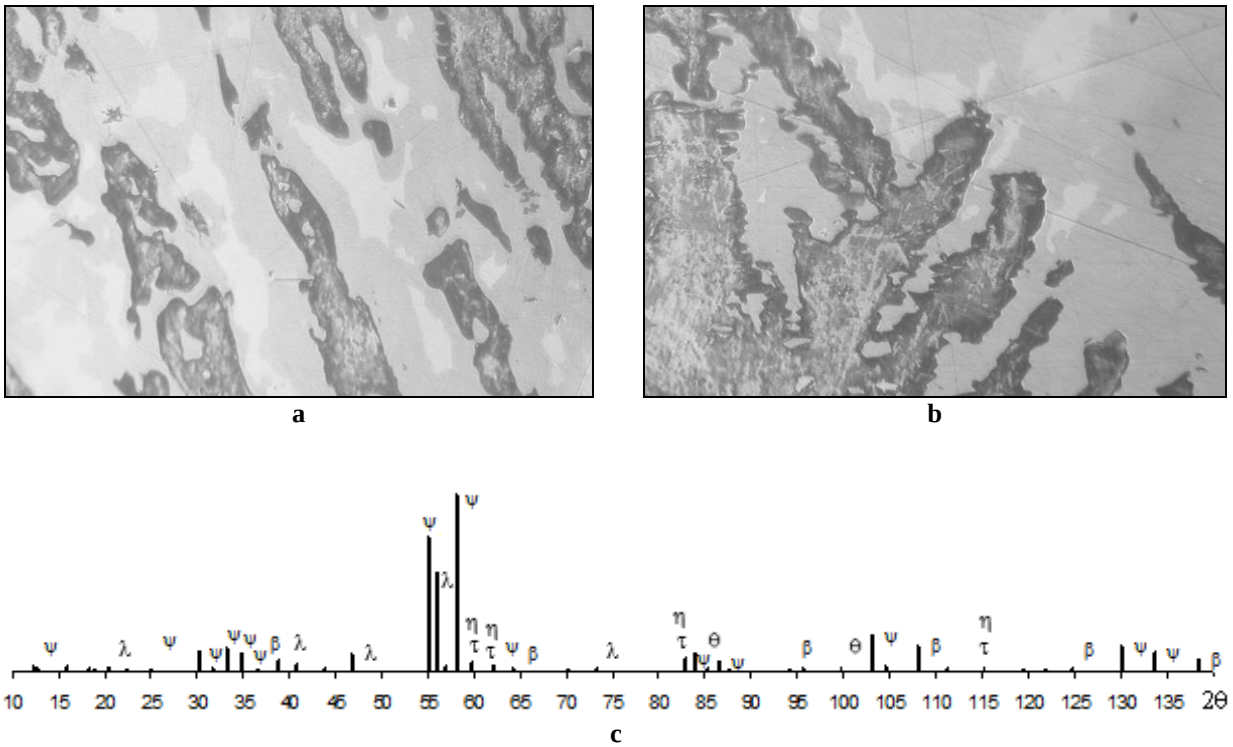

Fig. 1. The $Al_{63}Cu_{25}Fe_{12}$ alloy: a – OM image (x200); b – OM image (x400); c – XRD pattern.

quasicrystalline decagonal D-phase, crystalline $Al_4(Co,Cu)_3$ phase, crystalline $Al_3(Cu,Co)_2$ phase (Fig. 2,a) [4]. The described phase composition is confirmed by X-ray investigation (Fig. 2,b). After etching grey-colored quasicrystalline D-phase takes about 65 % of a total alloy volume. The solidification of the D-phase proceeds as a peritectic reaction, in which the primary $Al_4(Co,Cu)_3$ phase is surrounded by the D-phase. Subsequently $Al_3(Cu,Co)_2$ phase solidifies thus producing a three-phase peritectic structure.

Measurements evidence that the icosahedral and decagonal quasicrystals possess a microhardness of about 8.6 - 9.9 GPa [2, 4], which is much higher than that for crystalline phases. Comparison with the intermetallic compounds in the investigated alloys exhibits the following sequence:

$$H(\psi\text{-AlCuFe})>H(\text{D-AlCoCu})>H(Al_9(Co,Ni)_2)>$$
$$H(\lambda\text{-}Al_{13}Fe_4)>H(\tau\text{-AlCu(Fe)})>H(\theta\text{-}Al_2Cu).$$

Corrosion behavior of the icosahedral and decagonal quasicrystalline phases in the $Al_{63}Cu_{25}Fe_{12}$ and $Al_{63}Co_{24}Cu_{13}$ alloys is tested in 5 % NaCl solution which allows a comparison of their corrosion resistance under conditions comparable to application. Model immersion tests show that corrosion resistance of the $Al_{63}Cu_{25}Fe_{12}$ alloy is noticeably inferior to that of the $Al_{63}Co_{24}Cu_{13}$ alloy (Table 1). In a daytime, the surface of the $Al_{63}Cu_{25}Fe_{12}$ alloy loses its metallic luster, and gas bubbles appear here. Specific mass change (Δm) reaches 0.81 mg/cm^2. In a three-day time, the numerous corrosion damages and intensive gas evolution are observed on the surface. Corrosion products go partially into the solution and, therefore, the solution loses transparency. Eight days later, corrosion intensifies (Δm = 2.28 mg/cm^2). During the experiments, the pH of the working solution gradually increases which indicates that the sample corrodes under electrochemical mechanism with oxygen depolarization and formation of OH^- ions. Most likely, at the initial stage of corrosion, the surface iron atoms may be oxidized and act as anodes in galvanic couple. In contact with water and oxygen, the Fe^{2+} ions turn into Fe^{3+} ions. Final corrosion product observed visually on the surface is $xFe_2O_3{\cdot}yH_2O$ compound of non-stochiometric composition (brown rust). This layer formation is consistent with the change in color of the samples seen during the immersion.

The substitution of iron by cobalt in Al–Cu–Fe alloy is favorable for the essential increase of the corrosion resistance of the samples. After 8 days of the tests, the mass change of the $Al_{63}Co_{24}Cu_{13}$ alloy equals to 0.80 mg/cm^2 (Table 1). Only single gas bubbles are observed on the surface; color and transparency of working solution do not practically change. Gradual inhibition of a corrosion rate of the cobalt-containing alloy indicates that a passivation film consisted of corrosion products is formed during the tests. This film may be revealed visually as surface darkening that shows

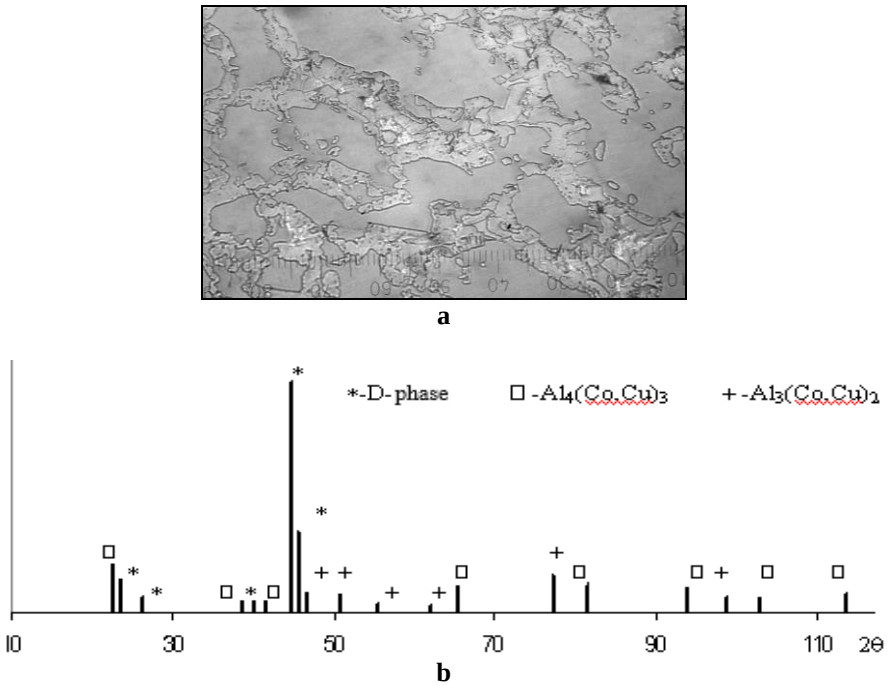

Fig. 2. The $Al_{63}Co_{24}Cu_{13}$ alloy: a – OM image (x400); b – XRD pattern.

Table 1

The specific mass change (in mg/cm^2) of $Al_{63}Co_{24}Cu_{13}$ and $Al_{63}Cu_{25}Fe_{12}$ alloys affected by 5-% NaCl solution

Alloy	Holding time, days				
	1	2	3	4	8
$Al_{63}Cu_{25}Fe_{12}$	0.81	1.39	1.47	2.28	2.74
$Al_{63}Co_{24}Cu_{13}$	0.12	0.48	0.65	0.72	0.80

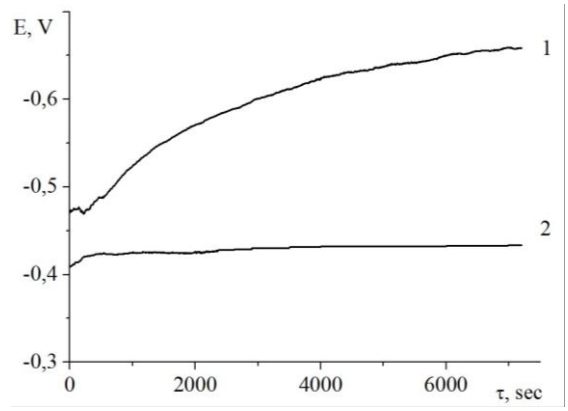

Fig. 3. (E,τ)-curves recorded for $Al_{63}Cu_{25}Fe_{12}$ (1) and $Al_{63}Co_{24}Cu_{13}$ (2) alloys in 5-% NaCl solution (pH = 7.0).

no color change of the surface with immersion duration. So, for the $Al_{63}Co_{24}Cu_{13}$ alloy, behavior is consistent with the formation of a passive layer.

The results of model immersion tests are in good agreement with chronopotentiometry measurements of free corrosion potentials (E) of the $Al_{63}Cu_{25}Fe_{12}$ and $Al_{63}Co_{24}Cu_{13}$ alloys in 5 % neutral NaCl solution. Fig. 3 shows that for $Al_{63}Cu_{25}Fe_{12}$ alloy a potential stabilizes at a value of –0.66 V during more than 7000 seconds (2 hours). For $Al_{63}Co_{24}Cu_{13}$ alloy, a potential has less negative value (–0.43 V) that stops changing no longer than after 1000 seconds of measurements. A rise of potential in the positive direction indicates the formation of a passive film and a steady potential indicates that the film remains intact and protective. So, as evidenced by obtained results, $Al_{63}Co_{24}Cu_{13}$ alloy is more corrosion resistant due to surface passivation. Polarization measurements confirm the chronopotentiometry results (Fig. 4).

In Fig. 4 are shown voltammograms recorded at potentials in the anodic direction from the stationary value up to a sharp increase of a current density due to oxidation of the alloys' constituents. After changing the direction of a potential sweep, in the cathodic area of a plot, the region of corrosion current limit is observed that is typical to corrosion processes with oxygen depolarization. At the reverse cycle of a potential sweep, the electrochemical passivity region may be determined. For $Al_{63}Cu_{25}Fe_{12}$ alloy this region extends from –1.0 V to –0.6 V, and for $Al_{63}Co_{24}Cu_{13}$ alloy from –1.0 V to –0.4 V. The extension of the passivity region towards more positive potentials indicates that the $Al_{63}Co_{24}Cu_{13}$ alloy is less susceptible to corrosion than the $Al_{63}Cu_{25}Fe_{12}$ alloy.

Fig. 5 shows the results of voltammetry presented in semi-logarithmic coordinates in order to determine corrosion current density (i). The intersection point of two plot branches corresponds to a logarithm of i. The

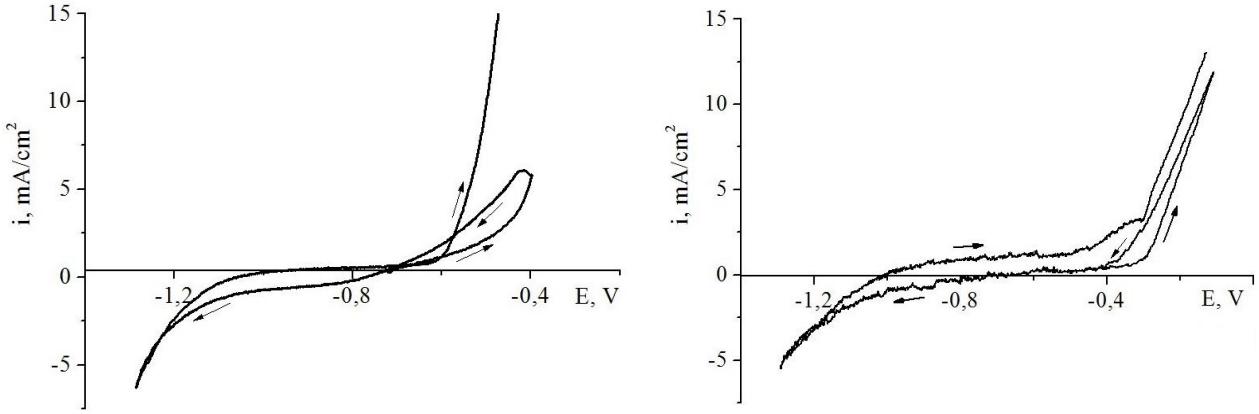

Fig. 4. Cyclic voltammograms recorded in 5-% NaCl solution (pH=7.0) for: a – $Al_{63}Cu_{25}Fe_{12}$; b – $Al_{63}Co_{24}Cu_{13}$ alloys.

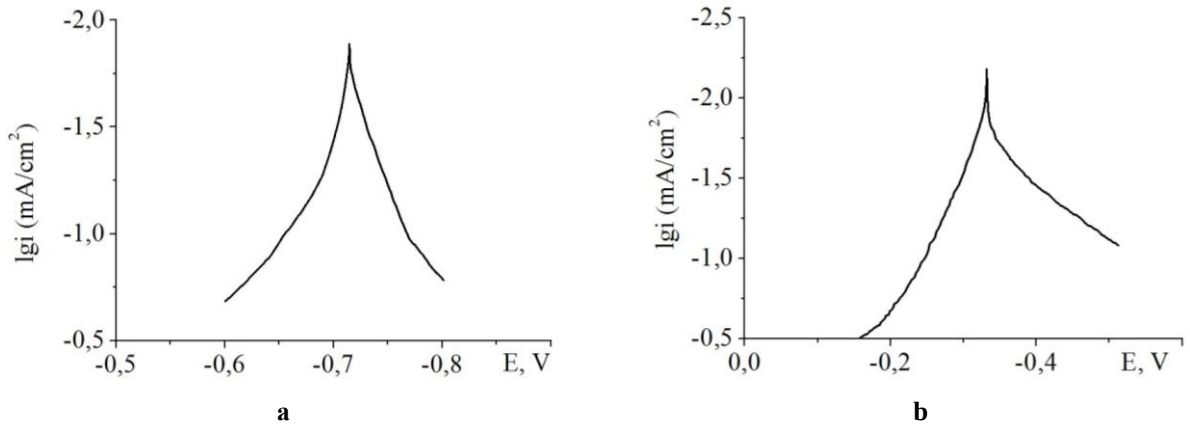

Fig. 5. (E,lg i)-curves recorded in 5-% NaCl solution (pH=7.0) for: a – $Al_{63}Cu_{25}Fe_{12}$; b – $Al_{63}Co_{24}Cu_{13}$ alloys.

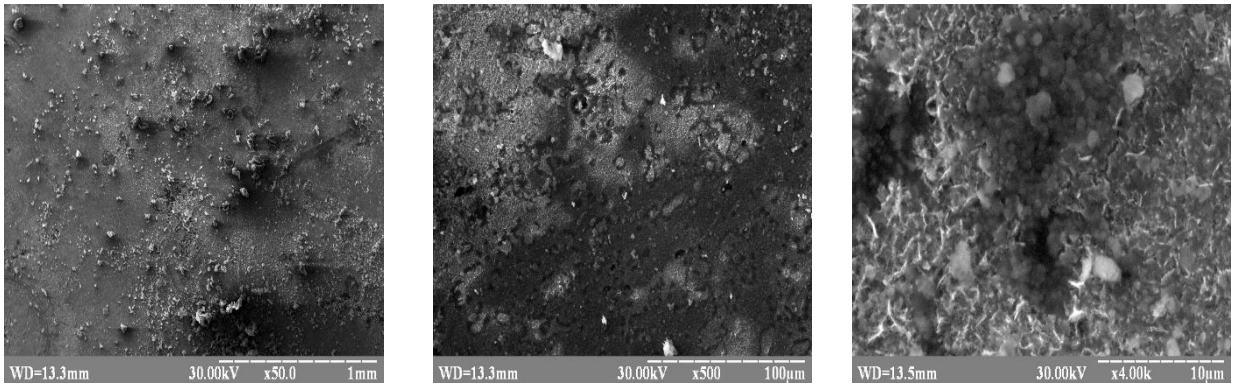

a **b** **c**

Fig. 6. SEM-images of the surface of $Al_{63}Cu_{25}Fe_{12}$ alloy after 8-day immersion test in 5-% NaCl solution (pH = 7.0).

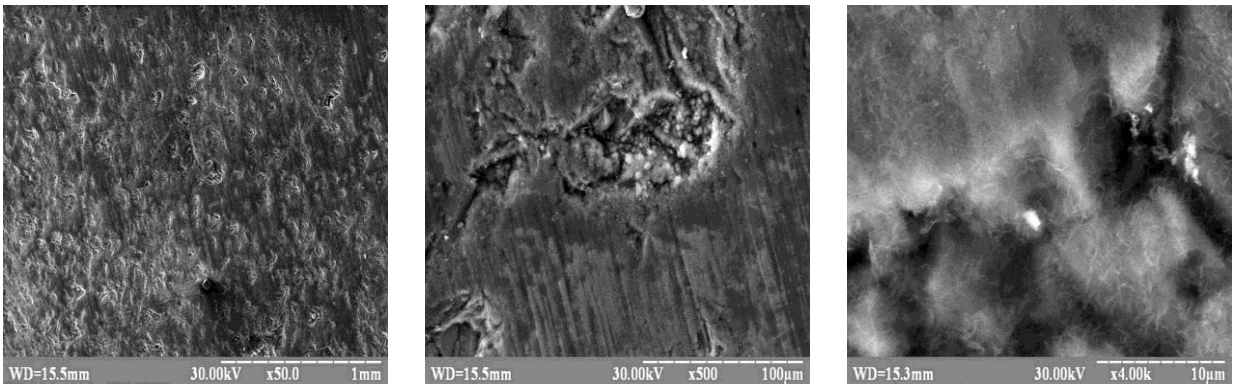

a **b** **c**

Fig. 7. SEM-images of the surface of $Al_{63}Co_{24}Cu_{13}$ alloy after 8-day immersion test in 5-% NaCl solution (pH = 7.0).

value of corrosion current density determined for the $Al_{63}Cu_{25}Fe_{12}$ alloy equals to 0.20 mA/cm^2 (Fig. 5,a), and that for the $Al_{63}Co_{24}Cu_{13}$ alloy is 0.18 mA/cm^2 (Fig. 5,b) which may relate to the inhibition of anodic processes for the $Al_{63}Co_{24}Cu_{13}$ alloy.

The SEM images of the surface of the $Al_{63}Cu_{25}Fe_{12}$ alloy corroded in 5 % sodium chloride solution evidence that after the 8-day tests pits are observed on the surface of the alloy (Fig. 6). Pits sites, sized from 10 to 50 μm, are non-uniformly distributed on the surface. Corrosion occurs primarily in the iron-rich λ-phase and secondarily in the quasicrystalline ψ-phase. The pits bottom is commonly covered by a porous layer of undissolved copper. The remains of non-separated brown rust are revealed on the alloy surface as well.

On the surface of $Al_{63}Co_{24}Cu_{13}$ alloy, pits about 10 μm in size located mainly in the vicinity of defects are also revealed (Fig. 7). In addition to pitting, the boundaries between the primary and peritectic phases are preferentially dissolved.

Thus, from the electrochemical point of view, the $Al_{63}Cu_{25}Fe_{12}$ and $Al_{63}Co_{24}Cu_{13}$ alloys behave quite similarly in the aqueous sodium chloride solution, but immersion tests show that on the surface of $Al_{63}Cu_{25}Fe_{12}$ alloy larger pits appear in greater quantity. So, a first order assessment would suggest that the $Al_{63}Cu_{25}Fe_{12}$ alloy has lower resistance to pitting than the $Al_{63}Co_{24}Cu_{13}$ alloy. The reason is that iron-rich phases and their boundaries in the structure of the $Al_{63}Cu_{25}Fe_{12}$ alloy are more susceptible to attack by saline solution. The pits on the surface of the $Al_{63}Cu_{25}Fe_{12}$ alloy are Cu-rich, apparently forming by dissolution of Fe and Al, and those on the surface of the $Al_{63}Co_{24}Cu_{13}$ alloy are Co- and Cu-rich due to preferential dissolution of Al. Hence, the general trend seems to be that the noblest metals remain at the surface during corrosion, while the other components, such as Fe and/or Al, dissolve. Corrosion is controlled mainly by chemical composition of the investigated alloys rather than the specific atomic structure of icosahedral or decagonal quasicrystalline phases present in their structure.

Conclusions

The investigations performed on conventionally solidified $Al_{63}Cu_{25}Fe_{12}$ and $Al_{63}Co_{24}Cu_{13}$ alloys confirm that both alloy systems cooled at 5 K/s form stable quasicrystalline icosahedral (ψ) and decagonal (D) phases correspondingly. In $Al_{63}Cu_{25}Fe_{12}$ alloy, the primarily solidified phase is λ-$Al_{13}Fe_4$ but, in $Al_{63}Co_{24}Cu_{13}$ alloy, the $Al_4(Co,Cu)_3$. Quasicrystalline ψ and D phases are further formed by peritectic reaction.

The corrosion of the investigated alloys in 5 % NaCl

aqueous solution (pH 6.9 - 7.1) occurs by the electrochemical mechanism with oxygen depolarization. More electropositive copper acts as cathode and more electronegative iron or cobalt – as anode.

When subjected to corrosion, iron-rich phases (λ and ψ) of $Al_{63}Cu_{25}Fe_{12}$ alloy selectively oxidize, with water soluble Fe^{2+} compounds forming. Affected by oxygen and water, these compounds turn into insoluble Fe^{3+} compounds that accumulate on the surface of the alloy and may partially separate from it.

As compared with $Al_{63}Cu_{25}Fe_{12}$ alloy, $Al_{63}Co_{24}Cu_{13}$ alloy shows better corrosion resistance which may relate to the formation of passive cobalt-containing compounds blocking the surface. This alloy has less negative free corrosion potential, wider electrochemical passivity region as well as scarcer and smaller pits on the surface affected by saline solution. Therefore, the $Al_{63}Co_{24}Cu_{13}$ alloy shows promise as a coating material to protect rocket-and-space equipment working in marine atmosphere.

Sukhova O.V. **–** Full Professor, Dr Sci Eng., Professor of Experimental Physics Chair;
Polonskyy V.A. **–** Associate Professor, PhD Chem., Associate Professor of Chair of Physical, Organic and Non-organic Chemistry.

[1] E. Huttunen-Saarivirta, Journal of Alloys and Compounds 363(1-2), 150 (2004) (https://doi.org/10.1016/S0925-8388(03)00445-6).
[2] O.V. Sukhova, K.V. Ustinova, Functional Materials 26(3), 495 (2019) (https://doi.org/10.15407/fm26.03.495).
[3] A.-P. Tsai, A. Inoue, T. Masumoto, Materials Transactions JIM 30(4), 300 (1989) (https://doi.org/10.2320/matertrans1989.30.300).
[4] O.V. Sukhova, Y.V. Syrovatko, Metallofizika i Noveishie Tekhnologii 41(9), 1171 (2019) (https://doi.org/10.15407/mfint.41.09.1171).
[5] S.S. Kang, J.M. Dubois, Journal of Materials Research 6(10), 2471 (1993) (https://doi.org/10.1557/jMR.1993.2471).
[6] R.P. Matthews, C.I. Lang, D. Shechtman, Tribology Letters 7, 179 (1999) (https://doi.org/10.1023/A:1019185707264).
[7] A. Rudiger, U. Koster, Materials Science and Engineering 294-296, 890 (2000) (https://doi.org/10.1016/S0921-5093(00)01037-6).
[8] E. Huttunen-Saarivirta, T. Tiainen, Materials Chemistry and Physics 85, 383 (2004) (https://doi.org/10.1016/j.matchemphys.2004.01.025).
[9] O.V. Sukhova, V.A. Polonskyy, K.V. Ustinova, Materials Science 55(2), 285 (2019) (https://doi.org/10.1007/s11003-019-00302-2).
[10] O.V. Sukhova, Metallofizika i Noveishie Tekhnologii 31(7), 1001 (2009).
[11] O.V. Sukhova, V.A. Polonskyy, K.V. Ustinova, Physics and Chemistry of Solid State 18(2), 222 (2017) (https://doi.org/10.15330/PCSS.18.2.222-227).
[12] G. Laplanche, A. Joulain, J. Bonneville, Journal of Alloys and Compounds 493, 453 (2010) (https://doi.org/10.1016/j.jallcom.2009.12.124).
[13] I.M. Spiridonova, O.V. Sukhova, A.P. Vashchenko, Metallofizika i Noveishie Tekhnologii 21(2), 122 (1999).
[14] I.M. Spyrydonova, O.V. Sukhova, G.V. Zinkovskij, Metallurgical and Mining Industry 4(4), 2 (2012).
[15] Z.A. Duriagina, T.M. Kovbasyuk, S.A. Bespalov, Uspekhi Fiziki Metallov 17(1), 29 (2016) (https://doi.org/10.15407/ufm.17.01.029).
[16] V.G. Efremenko, Yu.G. Chabak, A. Lekatou, A.E. Karantzalis, A.V. Efremenko, Metallurgical and Materials Transactions A 47A(2), 1529 (2016) (https://doi.org/10.1007/s11661-018-4722-0).
[17] C. Zhou, R. Cai, S. Gong, H. Xu, Surface Coating Technology 201, 1718 (2006) (https://doi.org/10.1016/j.surfcoat.2006.02.043).
[18] Y. Kang, C. Zhou, S. Gong, H. Xu, Materials Science Forum 475-479, 3355 (2005) (https://doi.org/10.4028/www.scientific.net/MSF.475-479.3355).
[19] I.M. Spiridonova, E.V. Sukhovaya, V.F. Butenko, A.P. Zhudra, A.I. Litvinenko, A.I. Belyi, Powder Metallurgy and Metal Ceramics 32(2), 139 (1993) (https://doi.org/10.1007/BF00560039).
[20] S.I. Ryabtsev, V.A. Polonskyy, O.V. Sukhova, Powder Metallurgy and Metal Ceramics 58(9-10), 567 (2020) (https://doi.org/10.1007/s11106-020-00111-2).
[21] S.I. Ryabtsev, O.V. Sukhova, Problems of Atomic Science and Technology 2(126), 145 (2020).

О.В. Сухова, В.А. Полонський

Закономірності структуроутворення та корозії литих квазікристалічних сплавів $Al_{63}Cu_{25}Fe_{12}$ та $Al_{63}Co_{24}Cu_{13}$ у водному розчині натрій хлориду

Дніпровський національний університет імені Олеся Гончара, Дніпро, Україна, sukhovaya@ukr.net

В роботі досліджено структуру і особливості корозії квазікристалічних литих сплавів $Al_{63}Cu_{25}Fe_{12}$ та $Al_{63}Co_{24}Cu_{13}$ в 5 %-ному розчині натрій хлориду (pH 6,9 - 7,1). Швидкість охолодження сплавів складала 5 К/с. Структуру сплавів вивчали методами кількісної металографії, рентгеноструктурного аналізу, растрової електронної мікроскопії. Корозійні властивості досліджували потенціодинамічним методом. Проведені дослідження підтверджують утворення стабільних квазікристалічних ікосаедричної (ψ) та декагональної (D) фаз у структурі сплавів $Al_{63}Cu_{25}Fe_{12}$ та $Al_{63}Co_{24}Cu_{13}$ відповідно. У 5 %-ному розчині натрій хлориду досліджені сплави кородують за електрохімічним механізмом з кисневою деполяризацією. Порівняно зі сплавом $Al_{63}Cu_{25}Fe_{12}$, сплав $Al_{63}Co_{24}Cu_{13}$ має менш від'ємні значення потенціалу вільної корозії (–0,43 В і –0,66 В відповідно), а його зона електрохімічної інертності розширюється за рахунок гальмування анодних процесів. Величина струму корозії, розрахована з (E, lgi)–залежностей, для сплаву $Al_{63}Co_{24}Cu_{13}$ складає 0,18 мА/см^2, а для сплаву $Al_{63}Cu_{25}Fe_{12}$ – 0,20 мА/см^2. Більш низьку корозійну тривкість сплаву $Al_{63}Cu_{25}Fe_{12}$ пояснено присутністю в його структурі залізовмістних фаз. Послуговуючись отриманими результатами, для створення покриттів на деталях ракетно-космічної техніки, що працюють в умовах морського клімату, рекомендовано сплав $Al_{63}Co_{24}Cu_{13}$.

Ключові слова: ікосаедричні квазікристали, декагональні квазікристали, структура, електрохімічна поляризація, пітінгова корозія.